Multi-block Polyesters Demonstrating High Elasticity and Shape Memory Effects

Yunqing Zhu, [1]Madalyn R. Radlauer,[2§] Deborah K. Schneiderman,[2] Milo S.P. Shaffer,[3] Marc A. Hillmyer[2], Charlotte K. Williams[1]*

1. Chemistry Research Laboratory, Department of Chemistry, University of Oxford, Oxford OX1 3TA, UK.

2. Department of Chemistry, University of Minnesota, Minneapolis, 55455-0431 USA.

3. Department of Chemistry, Imperial College London, London SW7 2AZ, UK.

§Current address for MRR: Department of Chemistry, San Jose State University, San Jose, CA, 95192-0101, USA.

Abstract

Polyester block polymers containing polylactide have garnered significant attention as renewable, degradable alternatives to traditional elastomers. However, the low glass transition of the PLA blocks limits the upper-use temperatures of the resulting elastomers. To improve the thermal performance, we explore a series of multi-block polyesters composed of poly(ε-decalactone) (PDL) and poly(cyclohexene phthalate) (PCHPE). These materials are prepared using switchable polymerization catalysis followed by chain extension, the strategy involves: i) alternating ring-opening copolymerization (ROCOP) of cyclohexene oxide and phthalic anhydride, ii) ε-decalactone ring-opening polymerization (ROP), and iii) isocyanate coupling of the telechelic triblocks to increase molar mass. The resulting multi-block polyesters are amorphous and the blocks are phase separated; glass transition temperatures are ~ -45 °C and 100 °C. They show thermal resistance to mass loss with $T_{d5\%}$ ~ 285 °C and higher upper use temperatures compared to alternative aliphatic polyesters. The nanoscale phase behaviour and correlated mechanical properties are highly sensitive to the block composition. The sample containing PCHPE = 26 wt% behaves as a thermoplastic elastomer with high elongation at break (ε_b > 2450%), moderate tensile strength (σ_b = 12 MPa) and low

residual strain (ε_r ~ 4%). It shows elastomeric behaviour from -45 to 100 °C and has a processing temperature range of ~170 °C. At higher PCHPE content (59 wt%), the material has shape memory character with high strain fixation (250%) and recovery (96%) over multiple (25) recovery cycles. The multi-block polyesters are straightforward to prepare and the methods presented here can be extended to produce a wide range of new materials using a other epoxides, anhydrides and lactones. This first report on the thermal and mechanical properties highlights the significant potential for this class of polyesters as elastomers, rigid plastics and shape memory materials.

Graphical abstract:

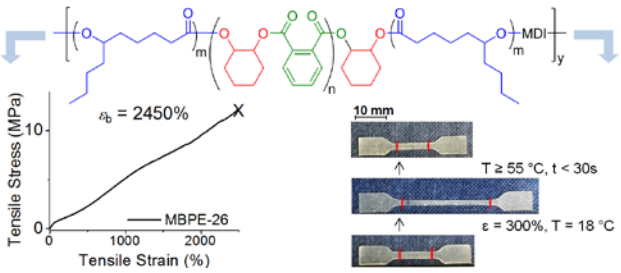

Introduction

Polymers are important chemical products that are manufactured at >300 Mt/annum worldwide.[1] They are used in almost every aspect of everyday life. However, their production does have environmental impacts: the manufacturing raw material and energy requirements consume ~8% of worldwide oil/gas reserves and their indiscriminate disposal can cause environmental pollution because they are pervasive. An important future challenge is to match, and improve upon, the properties of current materials whilst increasing sustainability and designing for degradation and recycling.[1-4] Currently, the largest scale sustainable industrial polymer is polylactide (PLA) which is sourced from high starch content crops such as corn/sugar beet and biodegrades, *via* ester bond hydrolysis, to the metabolite lactic acid.[5] Although PLA is applied in various packaging, fibre and medical applications, its properties fall short of those required for many other applications.[6]

Block polymers can undergo phase separation to form nanostructures showing improved macroscopic properties compared to homopolymer blends. For example, thermoplastic elastomers (TPE) are microphase separated block polymers used to replace rubber; typically they feature hard blocks of a glassy thermoplastic dispersed in a soft elastomeric matrix.[7] The soft blocks deliver elasticity whilst the hard blocks anchor the structure and mitigate creep. Block polymer TPEs are used in areas as diverse as household goods, automotive components, construction, medical devices/implants, drug delivery, tissue engineering, and electronics.[8-10] Generally thermoplastic elastomers are ABA triblock copolymers (where A = hard block and B = soft block); this configuration is considered optimal since it increases the hard block physical crosslinks which are important to the overall mechanical performance.

One widely used ABA triblock thermoplastic elastomer is polystyrene-*b*-polybutadiene-*b*-polystyrene (SBS) which exhibits high elasticity, moderate stress at break and operating windows as broad as −90 to 100 °C. Although widely applied, poly(styrene)-*b*-polyolefin-*b*-poly(styrene) materials are generally produced using conventional petrochemical raw materials; one alternative is to develop degradable block polymers which may even derive from renewable resources.[5,11-14]

Polyester thermoplastic elastomers are expected to be degradable by ester hydrolysis reactions, the rates of which depend on the precise structures. So far, various polyester thermoplastic elastomers have been investigated,[14-20] and whilst there are alternatives to the polyolefin soft-blocks,[21-27] the replacement of the polystyrene hard blocks presents a different challenge. In this context, semi-crystalline PLA has shown promise, for example, the triblock copolymer, [poly(L-lactide)-*b*-poly(*γ*-methyl-*ε*-caprolactone)-*b*-poly(L-lactide)] showed comparable toughness and elongation at break to SBS.[25] Nonetheless, polylactide derived thermoplastic elastomers are unsuitable for many applications requiring high temperature stability because PLA has only a moderate temperature stability and lower glass and melting transitions (T_g = 60 °C; T_m = 160 °C).[28] Block polyesters featuring main chain rigid or aromatic functional groups are expected to increase the thermoplastic glass transition temperature and are therefore important targets as alternative hard blocks.

PLA, and related aliphatic polyesters, are best produced using well-controlled lactone ring opening polymerization (ROP) which yields polyesters with predictable molar mass, narrow dispersity and a high fidelity of chain end groups.[29] Sequential lactone ROP reactions have been a very effective route to aliphatic block polyester thermoplastic elastomers.[14] In contrast, using lactone ROP to prepare semi-aromatic or rigid polyesters requires the

synthesis of new lactones.[30] Many such lactone syntheses require multi-step reactions that are difficult to scale and result in low overall yields.[30] Unfortunately, many aromatic/rigid functionalized lactones also show lower ring strain which reduces the thermodynamic driving force for polymerization.[30] Practically, the overall conversion is reduced and intermediary polymer purification steps are required to remove residual monomer. Recent advances in semi-aromatic polyester syntheses are interesting but have yet to be exploited to prepare discrete block polymers.[28,31-37]

On the other hand, the ring-opening copolymerization (ROCOP) of epoxides/anhydrides provides an alternative, well-controlled route to aliphatic, semi-aromatic or rigid polyesters.[38,39] Importantly, the ROCOP thermodynamic parameters are not significantly impacted by the use of functionalized, aromatic or rigid epoxides/anhydrides, and so a wide range of polyesters can be produced with very high monomer conversions and yields.[38-43] Many epoxides and anhydrides are also already industrially manufactured at significant scale and low cost which is expected to simplify larger-scale polymer synthesis. Most of these monomer candidates are sourced from petrochemicals but several are, or could be, bio-derived.[44-52] In the context of the current work, routes exist to make cyclohexene oxide from triglycerides and phthalic anhydride from carbohydrates, whilst ε-decalactone, can be sourced from castor oil.[53-56] One current limitation of ROCOP is that rather high catalyst loadings are required (0.2-1 mol% vs. monomer). As the reaction is a controlled polymerization, the corresponding polyester molar masses are lower than those from ROP reactions (ROCOP polyesters typically show $1000 < M_n < 30{,}000$ g/mol).[38,39] ROCOP functions efficiently in the presence of chain transfer agents, such as water or diols, and, under such conditions, results in high selectivity for hydroxy telechelic polyesters. The ability to prepare telechelics is essential to enable further chain extension reactions to produce multi-block polymers. So far,

the properties and uses of polyesters prepared using ROCOP are under-explored and studies are restricted to uses as polyols or macro-monomers.[38,39]

Recently, we reported a one-pot process using a single switchable catalyst to selectively enchain block polyesters from mixtures of epoxide, anhydride and lactone (Scheme 1).[57,58] The polymerization proceeds firstly by ROCOP and subsequently by ROP; it is highly selective for triblock polyester formation and proceeds with high monomer conversions and control. Here, the goal is to characterize the resulting block polyester thermal and mechanical properties so as to better understand potential elastomeric and shape memory applications.

Results

Multi-block Polyester (MBPE) Synthesis

Multi-block polyesters (MBPE) were synthesized by reaction of triblock polyester precursors with a diisocyanate. The triblock copolyester precursors were prepared, according to our previous report, by using a dizinc catalyst and mixtures of phthalic anhydride (PA), cyclohexene oxide (CHO) and ε-decalactone (ε-DL) (Scheme 1).[57,58] The method yields only BAB triblock poly(ε-decalactone)-*b*-poly(cyclohexene phthalate)-*b*-poly(ε-decalactone) (PDL-*b*-PCHPE-*b*-PDL) with the relative composition of the blocks controlled by monomer stoichometry (Scheme 1, Table 1). Importantly, the triblock polyesters feature only hydroxyl end-groups, i.e. telechelic triblocks.[58] To accelerate the rate of reaction the catalysis was conducted in neat epoxide. Even under these conditions, the selectivity is very high for the alternating co-polymer and there were no detectable ether linkages.[58] The excess epoxide was removed after synthesis of the triblock polymer; the polyester compositions, molar masses and dispersity (*Đ*) values were unchanged by this purification protocol (Figure S1).

Scheme 1. Preparation of the multi-block polyesters (MBPE) (for values of n, m and y see Table 1).

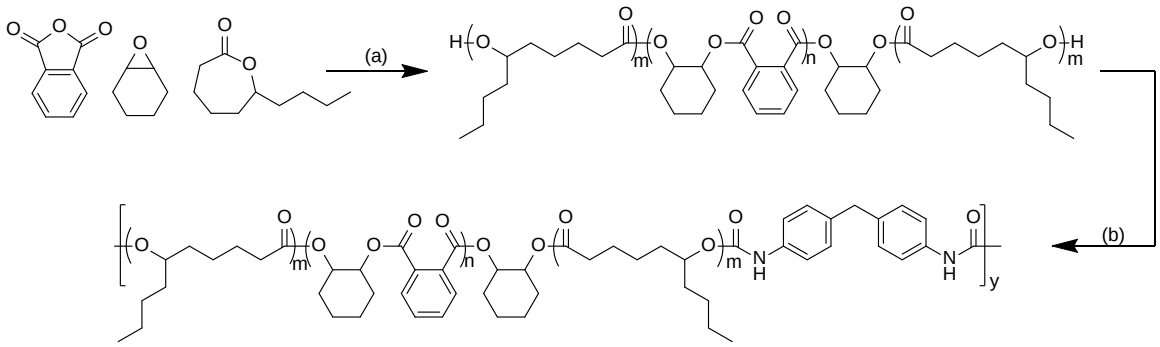

Reagents and conditions: (a) 1 equiv. [LZn_2Ph_2], 2 equiv. cyclohexane diol (CHD), 800 equiv. cyclohexene oxide (CHO), 100 equiv. phthalic anhydride (PA) and 100 equiv. ε-decalactone (ε-DL), 100 °C, 3.5 h.[58] See experimental section for further details and Figure S2 for the structure of [LZn_2Ph_2].[58,59] (b) 1.1 equiv. 4,4'-methylene diphenyl diisocyanate (MDI), 0.9 equiv. $Sn(Oct)_2$, toluene, 60 °C, 2 h.

The triblocks are hydroxy-telechelic so it is straightforward to carry out a post-polymerization chain extension by reaction with 4,4'-methylene diphenyl diisocyanate (MDI) which both increases molar mass and forms the desired structure of A blocks in the multi-block polyesters (MBPE-#, where # is the weight percentage of PCHPE block). The MBPEs have molar masses in the range 44–57 kg/mol and, on average, contain ~1 to 2 urethane linkages per chain (Table 1). As the coupling reaction is a step-growth process there may be residual triblock polyester in the multi-block polymers (*vide infra*).

Table 1. Multi-block polyester (MBPE) characterization data.

Sample[a]	{PDL$_m$-*b*-PCHPE$_n$-*b*-PDL$_m$-MDI}$_y$[c]			f_{PCHPE}[d]	$M_{n\ BAB}$ (kg/mol); $Đ$[e]	$M_{n\ MBPE}$ (kg/mol); $Đ$[e]	T_g (°C)[f]
	n	2m	y				
MBPE-26[b]	36	150	1.6	0.27	34.6; 1.19	56.6; 1.32	–49; N.A.

MBPE-42[b]	38	76	2.0	0.44	22.3; 1.22	44.8; 1.47	–47; 97
MBPE-49[b]	43	64	2.2	0.51	21.5; 1.16	47.4; 1.38	–43; 104
MBPE-59[b]	46	47	2.5	0.61	19.4; 1.21	48.1; 1.50	–42; 109
$(PDL)_y$[g]	0	93	1.9	0	15.9; 1.19	29.8; 1.67	–49; N.A.

[a] MBPE synthesis: See Scheme 1 and supporting information for details; [b] MBPE-#: # stands for the weight fraction of PCHPE (wt%) in MBPE. Determined using ^{1}H NMR spectroscopy by integration of peaks at 5.16 ppm (peak x) and 4.87 ppm (peak y); where the wt% PCHPE in MBPE=$[x\times(MW_{PA}+MW_{CHO})/(x+2y)]/\{[x\times(MW_{PA}+MW_{CHO})/(x+2y)]+[2y\times(MW_{DL})/(x+2y)]\}$; MW_{PA}, MW_{CHO} and MW_{DL} refer to the molar mass of PA, CHO and ε-DL, respectively; x and y stand for integrals, corresponding to peak x and y; [c] Determined using the following equations: $n = (M_{n,triblock}\times PCHPEwt\%)/(MW_{PA}+MW_{CHO})$; $2m = [M_{n,triblock}\times(100\% - PCHPEwt\%)]/(MW_{PA}+MW_{CHO})$; $y = M_{n,MBPE}/M_{n,triblock}$; MW_{PA} and MW_{CHO} refer to the molar mass of PA and CHO, respectively; [d] f_{PCHPE} was determined from the wt%(PCHPE) by using the room temperature density values for PDL (0.97 g·cm^{-3})[23] and PCHPE (1.04 ± 0.06 g·cm^{-3}, which was determined using a regular-shaped specimen. See supporting information for details); [e] Determined by SEC, in THF, using an RI detector calibrated using narrow dispersity polystyrene standards; [f] Acquired by DSC analysis from the second heating cycles, using a heating rate of 10 °C/min. The T_g values are reported as the midpoint of each transition (Fig. 1A); [g] Telechelic PDL was reacted with MDI yielding chain-extended $(PDL)_y$.

MBPE Microphase Separation

The multi-block copolymers were analysed by differential scanning calorimetry (DSC, values are determined from the second-heating cycle): only glass transition temperatures were observed. Most samples show two different T_g values which are close to the values for the two constituent polyesters ($T_{g\ PDL} \approx$ –58 °C,[53] $T_{g\ PCHPE} \approx$ 100 °C[60]). It is noteworthy that PCHPE shows a significantly higher T_g than alternative polyesters, such as polylactide ($T_g \approx$ 60 °C).[31,40,61,62] MBPE-26 showed only one T_g, at a temperature close to that of its majority PDL block, the second higher temperature transition is likely not observed due to the low

PCHPE content (Table 1 and Figure 1A). These results are consistent with the formation of amorphous and immiscible multi-block polyesters. DSC analyses did not show any evidence of urethane linkage crystallization, even after prolonged storage over several months. Moreover, the MBPEs did not show any sharp peaks in the wide-angle X-ray scattering (WAXS) analysis (at room temperature) either before or after thermal annealing (at 130 °C for 48 h); these findings are also consistent with the formation of fully amorphous materials (Figure S3).

Solvent cast samples of the MBPEs were analysed by small-angle X-ray scattering (SAXS) and transmission electron microscopy (TEM), at ambient temperature, to determine the nanoscale morphology. SAXS analysis showed principal scattering peaks for all MBPEs, consistent with phase separation, however, only MBPE-59 displayed any well-defined higher order peaks, indicating a lack of long-range order in most samples (Figure 1B).[63] The domain spacing values (d) obtained from the SAXS data were: 14 nm (MBPE-26), 12 nm (MBPE-42), 14 nm (MBPE-49) and 12 nm (MBPE-59). The samples were also investigated after thermal annealing, at 130 °C for 48 h, whereupon higher order peaks for MBPE-49 and MBPE-59 were observed indicating that thermal treatment increases long-range order (Figure S4). As control experiments, the equivalent SAXS analyses were conducted using films of the precursor triblocks; principal scattering peaks at similar spacings were observed suggesting phase separation without long-range order (Figure S5).

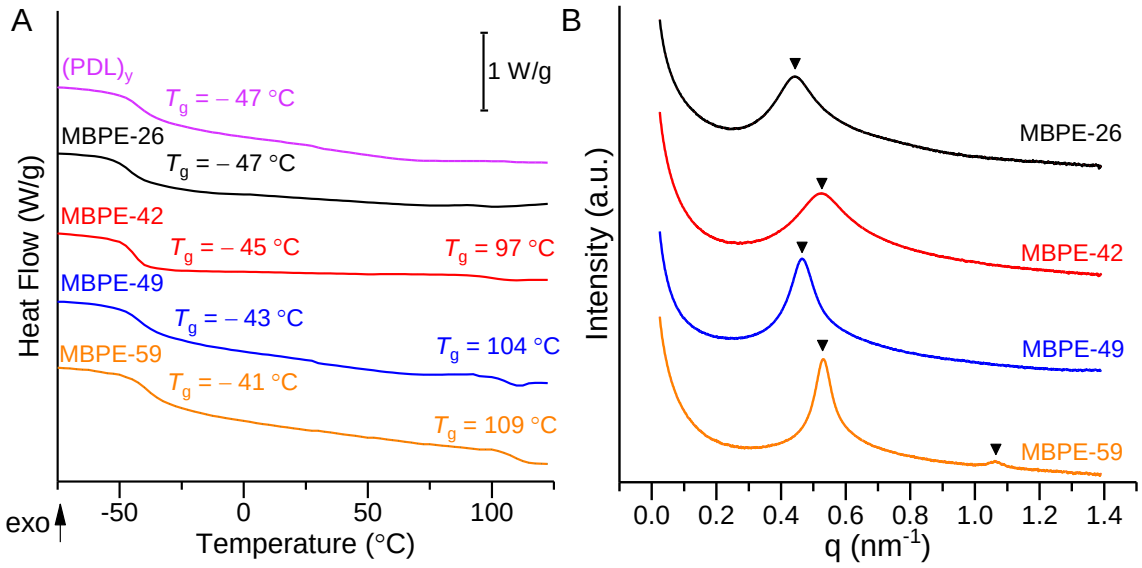

Figure 1. (A) DSC thermograms of the MBPEs and a control sample of chain extended PDL, $(PDL)_y$. The traces have been shifted vertically for clarity. The DSC chromatogram of the triblock polyesters are illustrated in Figure S8. (B) SAXS profiles of the MBPE samples, at ambient temperature (see Table 1, entries 1-4). Domain spacing (d) values are calculated ($d = 2\pi/q$) as 14 nm, 12 nm, 14 nm and 12 nm, respectively. The traces have been shifted vertically for clarity.

The phase separation was also confirmed by TEM analysis (bright field images in Figure S6 and the corresponding FFT analyses in Figure S7). The morphology changed according to the triblock composition, from worm-like PCHPE domains in a PDL matrix (MBPE-26) to worm-like PDL domains in a PCHPE matrix (MBPE-59). In line with SAXS measurements, the TEM images did not show any evidence of long-range order, even in the case of MBPE-59.

Temperature stability and thermo-mechanical analyses

Understanding the multi-block polyester temperature stability is relevant to inform polymer processing and applications. Thermogravimetric analysis (TGA) was used to assess thermal stability toward mass loss: all MBPEs showed similar decomposition behaviour and had

degradation temperatures (T_d corresponding to 5% mass loss) ~ 285 °C (Figure 2A). In comparison, amorphous PLA undergoes thermal degradation between 215-285 °C.[6] Overall, the difference between the rigid block T_g value (~100 °C) and the on-set of thermal degradation is at least 170 °C, which indicates a wide temperature range for processing.

The MBPEs were also examined by dynamic thermomechanical analysis (DMTA). Figure 2B shows the dynamic storage modulus (*E'*), loss modulus (*E''*) and tan(δ) as a function of temperature for MBPE-26. The DMTA analyses for MBPE-42, MBPE-49 and MBPE-59 are shown in Figure S9. All samples show similar trends: *E'* decreases drops from –45 to 0 °C, due to the softening of the PDL phase. MBPE-26 shows a rubbery plateau from 0 to 60 °C, with *E'* ~3 MPa. At higher temperatures, *E'* decreases somewhat and this is particularly apparent as the temperature approaches the T_g for the rigid block (PCHPE). There is a concurrent increase in tan δ indicating an increase in the mobility of some PCHPE chain segments at temperatures > 60 °C. For MBPE-26, the effect is small and unlikely to be disadvantageous to elastomer applications, but for the rigid plastic samples (MBPE-42 to 59) the effect is more significant. There is no crossover of *E'* and *E''* values up to 100 °C,[64] which confirms the hard block T_g determined by DSC and indicates that the material remains elastic from ca. −20 to 100 °C. Overall, MBPE-26 has a usable temperature range which is well aligned with many thermoplastic elastomer applications.[65]

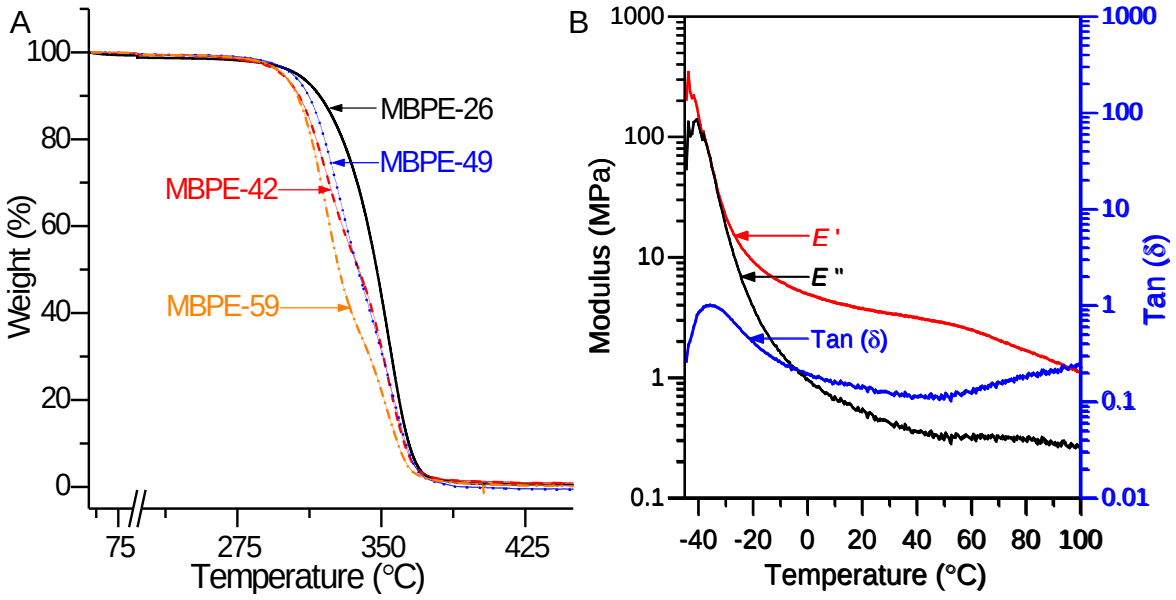

Figure 2. (A) TGA profiles of the MBPEs. (a) MBPE-26, T_d = 279 °C; (b) MBPE-42, T_d = 281 °C; (c) MBPE-49, T_d = 289 °C; (d) MBPE-59, T_d = 285 °C; T_d values are reported from the temperature at 5% mass loss. Heating rate: 20 °C/min. (B) Overlay of the storage modulus *E'*, loss modulus *E"* and tan(δ) of MBPE-26; conditions: ω = 1 Hz, strain = 1%, temperature ramp rate = 3 °C/min.

Mechanical Properties

The MBPE samples were each subjected to uniaxial extension experiments (10 mm/min): the materials show stress at break (σ_b) values from 12 to 17 MPa and elongations at break (ε_b) from 420 to 2450% (Figure 3A and Table 2). The tensile plots of those triblock precursors which formed suitable specimens are available in the supporting information (Figure S10 and Table S1). The mechanical properties are correlated with the block compositions and easily controlled through the starting monomer ratios. The three samples containing ≥ 42 wt% PCHPE showed plastic behaviour with distinct yield points in the stress-strain plots (Figure 3A, Table 2). MBPE-42 also showed a strain-induced plastic-to-rubber transition which is discussed in more detail in the supporting information (Figure S11).

In contrast, MBPE-26 does not show any clear yield point but rather behaves as a thermoplastic elastomer (TPE). Moreover, relative to a range of common commercial and literature polyester elastomers, it shows a high elongation at break which reaches 2450% (Table S2). Its elastic recovery was tested over 6 cycles of stretching to 200% strain, with a velocity of displacement of ±10 mm/min (cycles 1,2, and 6 are illustrated in Figure 3B). The Young's modulus and stress at constant strain both decrease slightly after the first cycle suggesting some plastic deformation and showing a residual strain $\varepsilon_r = 4 \pm 0.6\%$, typical behaviour for a thermoplastic elastomer.[66] After this first cycle, subsequent hysteresis cycles exhibit nearly identical behaviour and show no further increase in residual strain (Table S3). Thus, the sample appears to retain its physically crosslinked network even after being repeatedly deformed, which is attributed to its hard block rigidity and high T_g (~100 °C).[60]

To demonstrate the importance of the block polyester composition, a telechelic PDL homopolymer was chain extended by reaction with MDI to produce a chain extended analogue, $(PDL)_y$ (M_n = 29.8 kg/mol; Table 1). The resulting polymer could not retain its shape outside the mould and exhibited no elastomeric behaviour. Overall, MBPE-26 is an elastomer showing high elongation at break with low residual strain; its physical properties are consistent with its nanostructure whereby rigid PCHPE domains are present in a continuous PDL phase which underscores the importance of the multi-block architecture.

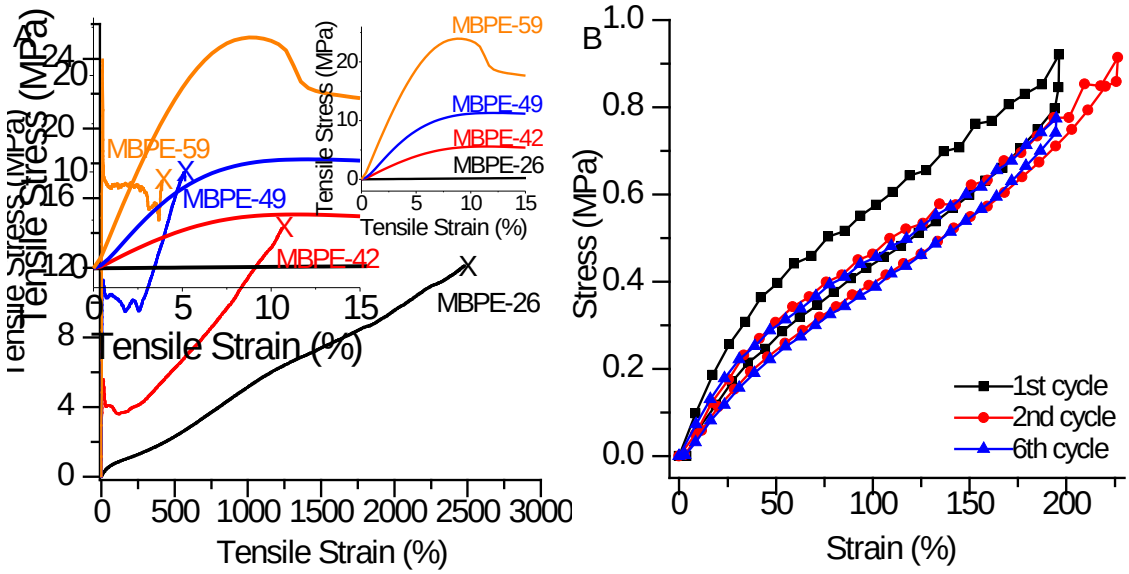

Figure 3. (A) Representative stress-strain curves for uniaxial extension of the multi-block polyesters MBPEs (Table 1). The failure points are marked with an 'X'. Inset: enlargement of the low strain region (0–15% strain). (B) Reversible hysteresis using sample MBPE-26. The sample was tested from 0– 200% strain, over 6 cycles, at a velocity of ±10 mm/min. The average residual strain after the first cycle is 4 ± 0.6% (Table S3).

Table 2. Mechanical properties of the MBPEs as a function of block composition.[a]

Sample	E_y[b] (MPa)	σ_b[c] (MPa)	ε_y[d] (%)	ε_b[e] (%)
MBPE-26	1.7 ± 0.6	12 ± 3	N.A.[b]	2450 ± 450
MBPE-42	78± 9	13 ± 6	19 ± 6	1200 ± 360
MBPE-49	180± 18	16± 6	12± 3	570 ± 180
MBPE-59	390 ± 9	17 ± 6	9 ± 6	420 ± 180

[a)] 95% confidence interval where the number of specimens is 3 in each case; [b)] Young's modulus; [c)] stress at break; [d)] strain at yield; [e)] elongation at break.

Shape Memory Polymer MBPE-59

MBPE-59 showed a shape memory effect. The tensile mechanical data show a significant plateau from 20–300% strain prior to the break point (Figure 3A). For rigid plastics such as MBPE-59, such a plateau is typically associated with cold-drawing where polymer segments

undergo orientation parallel to the applied force at temperatures below the glass transition.[67,68] Accordingly, the material remains deformed even after the external force is removed but may recover its shape when heated, particularly if heated above a glass (or melting) transition temperature.[67-70]

To investigate MBPE-59 further, a series of samples were stretched to 300% strain at ambient temperature (18 °C) and allowed to relax quiescently for 30 min, during which time only a slight retraction occurred and the fixed strain stabilized at ~ 280% for all samples. Next, the samples were each heated to various temperatures (35 °C, 55 °C, 75 °C, and 95 °C) and the resulting strain determined. No recovery was observed in the sample heated to 35 °C, but the samples heated to 55 °C showed near complete shape recovery within seconds and exhibited low residual strain (< 5%). Notably, this shape recovery behaviour at 55 °C occurs well below the glass transition temperature of pure PCHPE (T_g = 100 °C[60]) and that of the triblock precursor (T_g = 97 °C, Fig. S8). Furthermore, the recovery appears to be triggered abruptly at temperatures above 55 °C. To confirm the strain fixation at lower temperatures, a sample of MBPE-59 was stretched to 300% strain (at ambient temperature) and subsequently monitored over 6 weeks (again at ambient temperature): no significant change in strain fixity ratio was observed (see supporting information Eq. 1 and Figure S12). Nonetheless, when the sample was heated to 55 °C, near complete shape recovery occurred within seconds.

MBPE-59 was subjected to 25 stretching/recovery cycles to evaluate the shape memory behaviour (Figure 4 and supporting information for the experimental details). Throughout the entire 25 cycles, the shape-memory properties of MBPE-59 are retained and the material shows an average strain fixity of 91%. The absolute strain fixation is 250–290% (Figure 4A),

and the average strain recovery is~96 % (see supporting information eq.2). Photographs illustrating one stretching/recovery cycle of MBPE-59 are presented in Figure 4A.

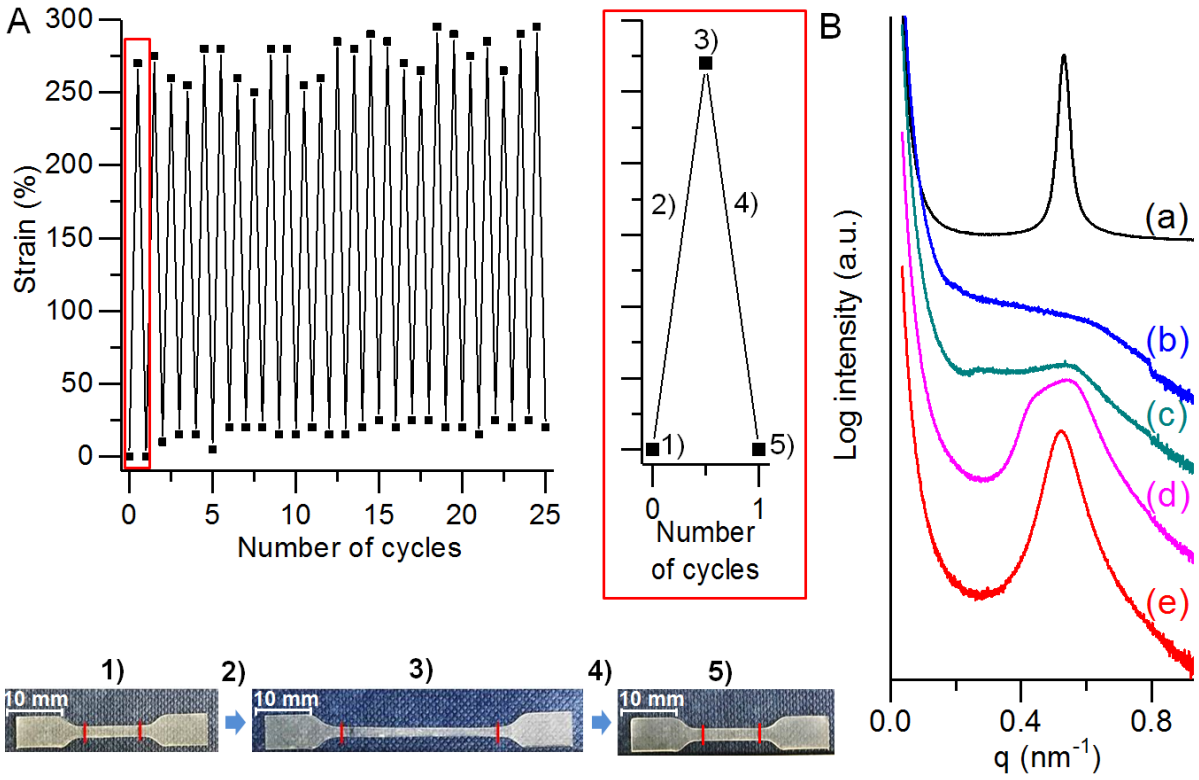

Figure 4. (A) Thermally--induced shape memory study using MBPE-59 over 25 cycles. Right: The first cycle, 1) original shape; 2) stretched to ε_{max} = 300%; 3) left to relax at 18 °C for 30 min; 4) heated to 55 °C to induce recovery; 5) shape recovered. Bottom: photographs of each stage of stretching and recovery of the sample. The gauge length is marked by red lines; (B) SAXS profiles of MBPE-59 during a stretching and recovery cycle. (a) as cast; (b) fully stretched (ε: 280%) at 18 °C; (c) partially recovered (residual ε: 185 %) at 55 °C, 10 s, then quenched in liquid N_2; (d) partially recovered (residual ε: 75 %) at 55 °C, 20 s, then quenched in liquid N_2; (e) fully recovered (residual ε: ~0 %) at 55 °C, 30 s, then quenched in liquid N_2. These samples were characterized at ambient temperature and the curves have been shifted vertically for clarity.

Changes in morphology during one shape memory cycle were monitored using SAXS (Figure 4B and supporting information). After the sample was stretched to 280%, the domain spacing decreased from 12 to 11 nm and the peak intensity reduced and broadened, such data

are indicative of changes in domain structure. Further characterization using 2D SAXS shows anisotropic scattering patterns (Figure S18). Similar effects were previously observed during cold-draw of microphase separated SBS or polystyrene-*b*-polyisoprene-*b*-polystyrene.[71-73] Next, the stretched sample of MBPE-59 was heated at 55 °C which triggered near complete shape recovery. SAXS analysis of the recovered sample showed a broader scattering peak compared to the original sample, but did confirm the return to the initial domain spacing (Figure 4B). The recovery of the original phase separated morphology was also confirmed by TEM analysis (Figure S19). MBPE-59 samples both before and after stretching were also examined by WAXS, the stretched sample shows a new low intensity, but sharp peak at q = 19.7 nm^{-1} (Figure S16). Further characterization using 2D WAXS was inconclusive (Figure S17).

To investigate the thermally triggered recovery process in more detail, a stretched sample of MBPE-59 ($\varepsilon \approx 280\%$) was analysed by DSC: in the first heating cycle, a low intensity endothermic peak was observed at ~50 °C. This peak was not observed in any subsequent heating cycles, suggesting it relates to a transition induced by the stretching process (Figure S13). The transition at ~50 °C was also observed when a stretched sample was analysed by DMTA (Figure S14). The moduli apparently increase at the transition, as the sample cross-section increases after relaxation of the shape memory strain. The small endotherm could be associated with some PCHPE melting interactions (see below), or simply the return to a higher entropy conformational state upon relaxation.

Samples MBPE-42 and MBPE-49 also showed shape memory effects but with reduced strain fixation and both demonstrated cold-draw only at limited strain values. The reduced performance of these samples may be caused by disruption of the rigid (PCHPE) phase into

individualized domains at high strain values, consistent with the strain induced plastic to rubber behaviour of MBPE-42 (see supporting information). Consequently, the high strain fixation needed for shape memory materials is only achieved for MBPE-59 which contains the highest content of rigid block. It is clear that sufficient rigid block content (PCHPE) is required to enable shape fixation by percolation of the rigid block across the network under shear. At temperatures above 50 °C, the mobility of some PCHPE chain segments likely triggers the shape recovery relaxation. A number of experiments were conducted in order to identify the specific molecular mechanism. The data were broadly consistent with various hypotheses to rationalize the shape recovery. The strained structure may be locked in place by the orientation of the PCHPE chains either through a low degree of strain induced crystallinity, or through local inter-chain interactions.[74] In both cases, the thermal trigger enables an energy barrier to chain relaxation to lower energy conformations. Another possibility is that there is a low degree of inter-domain solubility, such that at 50 °C the crucial points in the rigid network are sufficient plasticized to trigger shape recovery.[75] The possibility that residual triblock precursor present in the multi-block is directly responsible can be seemingly ruled out, since it shows a T_g only at 97 °C, close to that for the MBPE-59 (Figure S8). Furthermore, when residual triblock is present in significant concentration, it severely compromises mechanical performance (Figure S15).

Discussion

Thermoplastic elastomers

MPBE-26 has strength (σ_b = 12 ± 3 MPa) and stiffness (ε_b = 2450 ± 450 %) that are competitive with various commercial thermoplastic elastomers and with leading literature materials (Table S2).[18,19,24,76] Commercial thermoplastic elastomers typically show stress at break values 10–70 MPa with elongations at break < 900% (Table S2). For example, Styron

SPRINTA, an SBS elastomer, shows a stress at break of 19–22 MPa and elongations at break from 380–500% (Table S2, entry 8). MPBE-26 also shows competitive performance with various polyester/ether TPEs: Hytrel shows a stress at break of 10–30 MPa and elongation at break of 200–400% (Table S2, entry 1); Pibiflex shows stress at break of 10–40 MPa and elongation at break of 400–900% (Table S2, entry 4); and Kopel shows stress at break of 25–40 MPa and elongation at break of 400–850% (Table S2, entry 5).[65]

Polyester thermoplastic elastomers have also been widely explored in the academic literature, with significant research focussed on triblock polyesters based upon polylactide and other lactones.[14-17,77] Of direct relevance to this study are polylactide-*b*-poly(ε-decalactone)-*b*-polylactide and related block polyesters which are promising TPEs.[27,78] For example, high molar mass PLA-PDL-PLA triblock (M_n = 148 kg/mol) showed a stress at break of 9.4 MPa, with elongation at break of 1310%.[78] Multi-block polyesters prepared from the same monomers (LA/DL) showed better mechanical performances at lower molar masses than the triblocks with equivalent molar masses.[78] Here, MBPE-26 shows a higher or equivalent elasticity to other aliphatic polyesters but at lower molar mass (M_n = 57 kg/mol); the lower molar mass may be expected to facilitate sample processing. In contrast to the previously studied aliphatic polyesters, all prepared by sequential lactone ROP, MBPE-26 was synthesized by a switchable catalytic process using epoxide/anhydride/lactone mixtures. The catalysis proceeds in near quantitative yield (based on anhydride and lactone) and monomer conversion is very high, even at 100 °C. The results highlight the potential for switchable catalysis using other rigid epoxides/anhydrides/lactones to deliver improved performance thermoplastic elastomers and for use in blends to toughen brittle bio-based plastics.

Shape Memory Polymers

SMPs show promise for a range of applications including in medicine,[3] electronics[79,80] and as responsive textiles.[81] Various aliphatic block polyesters, including those containing blocks of semi-crystalline PCL[82-85] or PLA[86-88], show shape memory properties.[89-92] In the majority of cases, the semi-crystalline polyester blocks enable shape recovery to occur at temperatures exceeding the melting temperature,[93] although polyesters derived from bile acid were triggered by heating above a glass transition temperature.[94] Here, MBPE-59 shows distinctive and highly reproducible shape memory properties by using cold-draw to fix the temporary shape and with shaper recovery triggered by heating to ~ 55 °C, for a few seconds. Generally, cold-draw processing is an under-explored shape-memory programming method but is attractive as heating is not necessary to fix shape (and is only required in shape recovery).[3,93,95-101] One limitation of SMP cold-draw programming is that it usually affords low strain fixity ratios, values are typically well below 100%, and chemical crosslinking is required to increase strain fixity.[95,98] In contrast, here MBPE-59 shows high strain fixity and obviates the need for any further chemical processing. It also shows high absolute strain fixations (250–300%) which are at the upper end of values reported with typical SMP showing < 200%. [3,102-104] The average strain recovery of ~96% is also considerably higher than usual for physically crosslinked samples.[28,30]

Conclusions

The straightforward synthesis of a series of multi-block polyesters is reported *via* a combination of switchable polymerization catalysis, which links aliphatic and semi-aromatic block polyesters, followed by chain extension. The switchable catalysis is highly selective and is exploited to deliver multi-blocks with variable compositions and morphology which are either high elasticity thermoplastic elastomers, rigid plastics or shape memory polymers. The elastomer delivers high elasticity compared to other aliphatic polyesters and shows

competitive performance withsome commercial materials. It shows a wider usable temperature range – (ca. −20 to 100 °C) than previously reported polylactide based materials.

Overall this work demonstrates the potential for both the switchable catalysis and alternating semi-aromatic polyesters as high-performance materials. It is noteworthy that the one-pot catalytic method is particularly suited to the preparation of BAB type blocks; however, the interesting materials properties obtained suggest that it would worth exploring other routes to ABA system.More generally, there are many other anhydrides, epoxides, and lactones which could be polymerized using the methods described here to yield a very wide range of block polyesters and poly(ester-*b*-carbonates). The ability to use commercial monomers is important to facilitate polymer scale-up and may be expected to accelerate product implementation. Common commercially available monomers include vinyl-propylene oxide, vinyl-cyclohexene oxide, maleic anhydride or itaconic anhydride, all of which could also undergo post-polymerization reactions and/or cross-linking reactions to deliver more sophisticated and functional block polyesters. Finally, a wide range of bio-derived lactones/epoxides/anhydrides are known and should be targeted to make fully bio-based elastomers and shape-memory polymers.

Associated Content

Supporting Information: This material is available free of charge via the Internet at http://pubs.acs.org.

The supporting information contains NMR spectroscopy, differential scanning calorimetry, thermal gravimetric analysis, transmission electron microscopy, dynamic mechanical thermal analysis, X-ray scattering, tensile test and size exclusion chromatography data.

Author Information

Corresponding Author: charlotte.williams@chem.ox.ac.uk

CKW is a director and CSO of econic technologies.

Acknowledgments

The EPSRC (EP/L017393/1), EIT-Climate KIC (project EnCO2re), and the Imperial-CSC scholarship (to YZ) are acknowledged for funding. Partial support of this work was provided by the Center for Sustainable Polymers, a NSF-supported Center for Chemical Innovation (CHE- 1413862). We thank Dr. Matthew Irwin for assistance with the staining of TEM samples, Guilhem De Hoe and Dr. Alexander Todd for assistance with the tensile tests. SAXS measurements were performed at the DuPont-Northwestern-Dow Collaborative Access Team (DND-CAT) Synchrotron Research Centre located at Sector 5 of the Advanced Photon Source. DND-CAT is supported by the E.I. DuPont de Nemours & Co., The Dow Chemical Company, the U.S. National Science Foundation through Grant DMR-9304725, and the State of Illinois through the Department of Commerce and the Board of Higher Education Grant IBHE HECA NWU 96. Use of Advanced Photon Source was supported by the U.S. Department of Energy, Office of Science, Office of Basic Energy Science, under Contract No. W-31-109-Eng 38.

References

(1) Zhu, Y.; Romain, C.; Williams, C. K. Sustainable polymers from renewable resources. *Nature* **2016**, *540*, 354-362.
(2) Bates, F. S.; Hillmyer, M. A.; Lodge, T. P.; Bates, C. M.; Delaney, K. T.; Fredrickson, G. H. Multiblock Polymers: Panacea or Pandora's Box? *Science* **2012**, *336*, 434–440.
(3) Lendlein, A.; Kelch, S. Shape-Memory Polymers. *Angew. Chem. Int. Ed.* **2002**, *41*, 2034-2057.
(4) Fasolka, M. J.; Mayes, A. M. Block copolymer thin films: Physics and applications. *Ann. Rev. Mater. Res.* **2001**, *31*, 323-355.
(5) Hillmyer, M. A.; Tolman, W. B. Aliphatic Polyester Block Polymers: Renewable, Degradable, and Sustainable. *Acc. Chem. Res.* **2014**, *47*, 2390–2396.

(6) Auras, R.; Harte, B.; Selke, S. An overview of polylactides as packaging materials. *Macromol. Biosci.* **2004**, *4*, 835-864.
(7) Spontak, R. J.; Patel, N. P. Thermoplastic elastomers: fundamentals and applications. *Curr. Opin. Colloid. In.* **2000**, *5*, 334–341.
(8) Brannigan, R. P.; Dove, A. P. Synthesis, properties and biomedical applications of hydrolytically degradable materials based on aliphatic polyesters and polycarbonates. *Biomater. Sci.* **2017**, *5*, 9-21.
(9) Hillmyer, M. A.; Tolman, W. B. Aliphatic Polyester Block Polymers: Renewable, Degradable, and Sustainable. *Acc. Chem. Res.* **2014**, *47*, 2390–2396.
(10) Liu, Q. Y.; Jiang, L.; Shi, R.; Zhang, L. Q. Synthesis, preparation, in vitro degradation, and application of novel degradable bioelastomers-A review. *Prog. Polym. Sci.* **2012**, *37*, 715-765.
(11) Huang, Y.; Chang, R.; Han, L.; Shan, G.; Bao, Y.; Pan, P. ABA-Type Thermoplastic Elastomers Composed of Poly(ε-caprolactone-co-δ-valerolactone) Soft Midblock and Polymorphic Poly(lactic acid) Hard End blocks. *ACS Sustainable Chem. Eng.* **2016**, *4*, 121-128.
(12) Ghassemi, H.; Schiraldi, D. A. Thermoplastic Elastomers Derived from Bio-Based Monomers. *J. Appl. Polym. Sci.* **2014**, *131*.
(13) Gandini, A.; Lacerda, T. M. From monomers to polymers from renewable resources: Recent advances. *Prog. Polym. Sci.* **2015**, *48*, 1-39.
(14) Schneiderman, D. K.; Hillmyer, M. A. Aliphatic Polyester Block Polymer Design. *Macromolecules* **2016**, *49*, 2419-2428.
(15) Harrane, A.; Leroy, A.; Nouailhas, H.; Garric, X.; Coudane, J.; Nottelet, B. PLA-based biodegradable and tunable soft elastomers for biomedical applications. *Biomed. Mater.* **2011**, *6*, 11.
(16) Lee, S.; Yuk, J. S.; Park, H.; Kim, Y. W.; Shin, J. Multiblock Thermoplastic Elastomers Derived from Biodiesel, Poly(propylene glycol), and L-Lactide. *ACS Sustainable Chem. Eng.* **2017**, *5*, 8148-8160.
(17) Jaso, V.; Cvetinov, M.; Rakic, S.; Petrovic, Z. S. Bio-Plastics and Elastomers from Polylactic Acid/Thermoplastic Polyurethane Blends. *J. Appl. Polym. Sci.* **2014**, *131*, 8.
(18) Bolton, J. M.; Hillmyer, M. A.; Hoye, T. R. Sustainable Thermoplastic Elastomers from Terpene-Derived Monomers. *ACS Macro Lett.* **2014**, *3*, 717–720.
(19) Martello, M. T.; Hillmyer, M. A. Polylactide-Poly(6-methyl-epsilon-caprolactone)-Polylactide Thermoplastic Elastomers. *Macromolecules* **2011**, *44*, 8537–8545.
(20) Lee, S.; Lee, K.; Jang, J.; Choung, J. S.; Choi, W. J.; Kim, G. J.; Kim, Y. W.; Shin, J. Sustainable poly(epsilon-decalactone)-poly(L-lactide) multiarm star copolymer architectures for thermoplastic elastomers with fixed molar mass and block ratio. *Polymer* **2017**, *112*, 306-317.
(21) Wanamaker, C. L.; O'Leary, L. E.; Lynd, N. A.; Hillmyer, M. A.; Tolman, W. B. Renewable-resource thermoplastic elastomers based on polylactide and polymenthide. *Biomacromolecules* **2007**, *8*, 3634-3640.
(22) Wanamaker, C. L.; Bluemle, M. J.; Pitet, L. M.; O'Leary, L. E.; Tolman, W. B.; Hillmyer, M. A. Consequences of Polylactide Stereochemistry on the Properties of Polylactide-Polymenthide-Polylactide Thermoplastic Elastomers. *Biomacromolecules* **2009**, *10*, 2904-2911.
(23) Martello, M. T.; Schneiderman, D. K.; Hillmyer, M. A. Synthesis and Melt Processing of Sustainable Poly(epsilon-decalactone)-block-Poly(lactide) Multiblock Thermoplastic Elastomers. *ACS Sustainable Chem. Eng.* **2014**, *2*, 2519-2526.

(24) Xiong, M. Y.; Schneiderman, D. K.; Bates, F. S.; Hillmyer, M. A.; Zhang, K. C. Scalable production of mechanically tunable block polymers from sugar. *Proc. Natl. Acad. Sci. U. S. A.* **2014**, *111*, 8357–8362.
(25) Watts, A.; Kurokawa, N.; Hillmyer, M. A. Strong, Resilient, and Sustainable Aliphatic Polyester Thermoplastic Elastomers. *Biomacromolecules* **2017**, *18*, 1845-1854.
(26) Yang, J.; Lee, S.; Choi, W. J.; Seo, H.; Kim, P.; Kim, G. J.; Kim, Y. W.; Shin, J. Thermoset Elastomers Derived from Carvomenthide. *Biomacromolecules* **2015**, *16*, 246-256.
(27) Schneiderman, D. K.; Hill, E. M.; Martello, M. T.; Hillmyer, M. A. Poly(lactide)-block-poly(epsilon-caprolactone-co-epsilon-decalactone)-block-poly(lactide) copolymer elastomers. *Polym. Chem.* **2015**, *6*, 3641-3651.
(28) Baker, G. L.; Vogel, E. B.; Smith, M. R. Glass Transitions in Polylactides. *Polym. Rev.* **2008**, *48*, 64-84.
(29) Albertsson, A. C.; Varma, I. K. *Aliphatic polyesters: Synthesis, properties and applications*; Springer Berlin Heidelberg, 2002; Vol. 157.
(30) Pounder, R. J.; Dove, A. P. Towards poly(ester) nanoparticles: recent advances in the synthesis of functional poly(ester)s by ring-opening polymerization. *Polym. Chem.* **2010**, *1*, 260-271.
(31) Van Zee, N. J.; Coates, G. W. Alternating copolymerization of dihydrocoumarin and epoxides catalyzed by chromium salen complexes: a new route to functional polyesters. *Chem. Commun.* **2014**, *50*, 6322–6325.
(32) Lizundia, E.; Makwana, V. A.; Larranaga, A.; Vilas, J. L.; Shaver, M. P. Thermal, structural and degradation properties of an aromatic-aliphatic polyester built through ring-opening polymerisation. *Polym. Chem.* **2017**, *8*, 3530-3538.
(33) Fukuda, S.; Matsumura, S. Enzymatic Synthesis and Chemical Recycling of Aromatic Polyesters via Cyclic Oligomers. *Kobunshi Ronbunshu* **2011**, *68*, 332-340.
(34) Morales-Huerta, J. C.; Ciulik, C. B.; de Ilarduya, A. M.; Munoz-Guerra, S. Fully bio-based aromatic-aliphatic copolyesters: poly(butylene furandicarboxylate-co-succinate)s obtained by ring opening polymerization. *Polym. Chem.* **2017**, *8*, 748-760.
(35) Liu, T.; Simmons, T. L.; Bohnsack, D. A.; Mackay, M. E.; Smith, M. R.; Baker, G. L. Synthesis of Polymandelide: A Degradable Polylactide Derivative with Polystyrene-like Properties. *Macromolecules* **2007**, *40*, 6040-6047.
(36) Buchard, A.; Carbery, D. R.; Davidson, M. G.; Ivanova, P. K.; Jeffery, B. J.; Kociok-Kohn, G. I.; Lowe, J. P. Preparation of Stereoregular Isotactic Poly(mandelic acid) through Organocatalytic Ring-Opening Polymerization of a Cyclic O-Carboxyanhydride. *Angew. Chem. Int. Ed.* **2014**, *53*, 13858-13861.
(37) Sun, Y. Y.; Jia, Z. W.; Chen, C. J.; Cong, Y.; Mao, X. Y.; Wu, J. C. Alternating Sequence Controlled Copolymer Synthesis of alpha-Hydroxy Acids via Syndioselective Ring-Opening Polymerization of O-Carboxyanhydrides Using Zirconium/Hafnium Alkoxide Initiators. *J. Am. Chem. Soc.* **2017**, *139*, 10723-10732.
(38) Paul, S.; Zhu, Y.; Romain, C.; Brooks, R.; Saini, P. K.; Williams, C. K. Ring-opening copolymerization (ROCOP): synthesis and properties of polyesters and polycarbonates. *Chem. Commun.* **2015**, *51*, 6459-6479.
(39) Longo, J. M.; Sanford, M. J.; Coates, G. W. Ring-Opening Copolymerization of Epoxides and Cyclic Anhydrides with Discrete Metal Complexes: Structure-Property Relationships. *Chem. Rev.* **2016**, *116*, 15167-15197.
(40) Nejad, E. H.; Paoniasari, A.; van Melis, C. G. W.; Koning, C. E.; Duchateau, R. Catalytic Ring-Opening Copolymerization of Limonene Oxide and Phthalic Anhydride: Toward Partially Renewable Polyesters. *Macromolecules* **2013**, *46*, 631–637.
(41) Van Zee, N. J.; Coates, G. W. Alternating Copolymerization of Propylene Oxide with Biorenewable Terpene-Based Cyclic Anhydrides: A Sustainable Route to Aliphatic

Polyesters with High Glass Transition Temperatures. *Angew. Chem. Int. Ed.* **2015**, *54*, 2665-2668.
(42) Nejad, E. H.; van Melis, C. G. W.; Vermeer, T. J.; Koning, C. E.; Duchateau, R. Alternating Ring-Opening Polymerization of Cyclohexene Oxide and Anhydrides: Effect of Catalyst, Cocatalyst, and Anhydride Structure. *Macromolecules* **2012**, *45*, 1770-1776.
(43) Darensbourg, D. J.; Poland, R. R.; Escobedo, C. Kinetic Studies of the Alternating Copolymerization of Cyclic Acid Anhydrides and Epoxides, and the Terpolymerization of Cyclic Acid Anhydrides, Epoxides, and CO2 Catalyzed by (salen)(CrCl)-Cl-III. *Macromolecules* **2012**, *45*, 2242-2248.
(44) Sanford, M. J.; Carrodeguas, L. P.; Van Zee, N. J.; Kleij, A. W.; Coates, G. W. Alternating Copolymerization of Propylene Oxide and Cyclohexene Oxide with Tricyclic Anhydrides: Access to Partially Renewable Aliphatic Polyesters with High Glass Transition Temperatures. *Macromolecules* **2016**, *49*, 6394-6400.
(45) Van Zee, N. J.; Sanford, M. J.; Coates, G. W. Electronic Effects of Aluminum Complexes in the Copolymerization of Propylene Oxide with Tricyclic Anhydrides: Access to Well-Defined, Functionalizable Aliphatic Polyesters. *J. Am. Chem. Soc.* **2016**, *138*, 2755-2761.
(46) Carrodeguas, L. P.; Martin, C.; Kleij, A. W. Semiaromatic Polyesters Derived from Renewable Terpene Oxides with High Glass Transitions. *Macromolecules* **2017**, *50*, 5337-5345.
(47) Stosser, T.; Li, C. L.; Unruangsri, J.; Saini, P. K.; Sablong, R. J.; Meier, M. A. R.; Williams, C. K.; Koning, C. Bio-derived polymers for coating applications: comparing poly(limonene carbonate) and poly (cyclohexadiene carbonate). *Polym. Chem.* **2017**, *8*, 6099-6105.
(48) Carrodeguas, L. P.; Gonzalez-Fabra, J.; Castro-Gomez, F.; Bo, C.; Kleij, A. W. Al-III-Catalysed Formation of Poly(limonene)carbonate: DFT Analysis of the Origin of Stereoregularity. *Chem. Eur. J.* **2015**, *21*, 6115-6122.
(49) Hauenstein, O.; Reiter, M.; Agarwal, S.; Rieger, B.; Greiner, A. Bio-based polycarbonate from limonene oxide and CO2 with high molecular weight, excellent thermal resistance, hardness and transparency. *Green Chem.* **2016**, *18*, 760-770.
(50) Li, C. L.; Sablong, R. J.; Koning, C. E. Chemoselective Alternating Copolymerization of Limonene Dioxide and Carbon Dioxide: A New Highly Functional Aliphatic Epoxy Polycarbonate. *Angew. Chem. Int. Ed.* **2016**, *55*, 11572-11576.
(51) Auriemma, F.; De Rosa, C.; Di Caprio, M. R.; Di Girolamo, R.; Ellis, W. C.; Coates, G. W. Stereocomplexed Poly(Limonene Carbonate): A Unique Example of the Cocrystallization of Amorphous Enantiomeric Polymers. *Angew. Chem. Int. Ed.* **2015**, *54*, 1215-1218.
(52) Poland, S. J.; Darensbourg, D. J. A quest for polycarbonates provided via sustainable epoxide/CO2 copolymerization processes. *Green Chem.* **2017**, *19*, 4990-5011.
(53) Lin, J.-O.; Chen, W.; Shen, Z.; Ling, J. Homo- and Block Copolymerizations of ε-Decalactone with l-Lactide Catalyzed by Lanthanum Compounds. *Macromolecules* **2013**, *46*, 7769–7776.
(54) Winkler, M.; Romain, C.; Meier, M. A. R.; Williams, C. K. Renewable polycarbonates and polyesters from 1,4-cyclohexadiene. *Green Chem.* **2015**, *17*, 300–306.
(55) Mahmoud, E.; Watson, D. A.; Lobo, R. F. Renewable production of phthalic anhydride from biomass-derived furan and maleic anhydride. *Green Chem.* **2014**, *16*, 167–175.
(56) Giarola, S.; Romain, C.; Williams, C. K.; Hallett, J. P.; Shah, N. Techno-economic assessment of the production of phthalic anhydride from corn stover. *Chem. Eng. Res. Des.* **2016**, *107*, 181-194.

(57) Romain, C.; Zhu, Y.; Dingwall, P.; Paul, S.; Rzepa, H. S.; Buchard, A.; Williams, C. K. Chemoselective Polymerizations from Mixtures of Epoxide, Lactone, Anhydride, and Carbon Dioxide. *J. Am. Chem. Soc.* **2016**, *138*, 4120-4131.
(58) Zhu, Y.; Romain, C.; Williams, C. K. Selective Polymerization Catalysis: Controlling the Metal Chain End Group to Prepare Block Copolyesters. *J. Am. Chem. Soc.* **2015**, *137*, 12179–12182.
(59) Romain, C.; Garden, J. A.; Trott, G.; Buchard, A.; White, A. J. P.; Williams, C. K. Di-Zinc-Aryl Complexes: CO2 Insertions and Applications in Polymerisation Catalysis. *Chem. Eur. J.* **2017**, *23*, 7367-7376.
(60) Saini, P. K.; Romain, C.; Zhu, Y.; Williams, C. K. Di-magnesium and zinc catalysts for the copolymerization of phthalic anhydride and cyclohexene oxide. *Polym. Chem.* **2014**, *5*, 6068-6075.
(61) DiCiccio, A. M.; Coates, G. W. Ring-Opening Copolymerization of Maleic Anhydride with Epoxides: A Chain-Growth Approach to Unsaturated Polyesters. *J. Am. Chem. Soc.* **2011**, *133*, 10724–10727.
(62) Jeske, R. C.; DiCiccio, A. M.; Coates, G. W. Alternating copolymerization of Epoxides and cyclic anhydrides: An improved route to aliphatic polyesters. *J. Am. Chem. Soc.* **2007**, *129*, 11330–11331.
(63) Shin, J.; Lee, Y.; Tolman, W. B.; Hillmyer, M. A. Thermoplastic Elastomers Derived from Menthide and Tulipalin A. *Biomacromolecules* **2012**, *13*, 3833–3840.
(64) Mezger, T. G. *The Rheology Handbook*; Vincentz Network: Hannover, 2011.
(65) Fakirov, S. *Handbook of Condensation Thermoplastic Elastomers*; WILEY-VCH Verlag GmbH & Co. KGaA: Weinheim, 2005.
(66) Frick, E. M.; Zalusky, A. S.; Hillmyer, M. A. Characterization of Polylactide-*b*-polyisoprene-*b*-polylactide Thermoplastic Elastomers. *Biomacromolecules* **2003**, *4*, 216-223.
(67) Vinogradov, G. V.; Ya. Malkin, A.; Volosevitch, V. V.; Shatalov, V. P.; Yudin, V. P. Flow, high-elastic (recoverable) deformation, and rupture of uncured high molecular weight linear polymers in uniaxial extension. *J. Polym. Sci., Part B : Polym. Phys.* **1975**, *13*, 1721–1735.
(68) Pokrovskii, V. N. Contribution to the theory of forced high-elastic deformation of polymer materials. *Polym. Mech.* **1968**, *4*, 189–195.
(69) Vincent, P. I. The necking and cold-drawing of rigid plastics. *Polymer* **1960**, *1*, 7–19.
(70) Bower, D. *An Introduction to Polymer Physics*; Cambridge University Press, 2002.
(71) Honeker, C. C.; Thomas, E. L.; Albalak, R. J.; Hajduk, D. A.; Gruner, S. M.; Capel, M. C. Perpendicular deformation of a near-single-crystal triblock copolymer with a cylindrical morphology. 1. Synchrotron SAXS. *Macromolecules* **2000**, *33*, 9395-9406.
(72) Hashimoto, T.; Fujimura, M.; Saijo, K.; Kawai, H.; Diamant, J.; Shen, M. In *Multiphase Polymers*; American Chemical Society: 1979; Vol. 176, p 257–275.
(73) Prasman, E.; Thomas, E. L. High-strain tensile deformation of a sphere-forming triblock copolymer/mineral oil blend. *J. Polym. Sci., Part B: Polym. Phys.* **1998**, *36*, 1625–1636.
(74) Trznadel, M.; Kryszewski, M. Thermal Shrinkage of Oriented Polymers. *J. Macromol. Sci. R. M. C.* **1992**, *C32*, 259-300.
(75) Sobota, M.; Jurczyk, S.; Kwiecień, M.; Smola-Dmochowska, A.; Musioł, M.; Domański, M.; Janeczek, H.; Kawalec, M.; Kurcok, P. Crystallinity as a tunable switch of poly(L-lactide) shape memory effects. *J. Mech. Behav. Biomed. Mater.* **2017**, *66*, 144-151.
(76) Wang, Z.; Yuan, L.; Trenor, N. M.; Vlaminck, L.; Billiet, S.; Sarkar, A.; Du Prez, F. E.; Stefik, M.; Tang, C. Sustainable thermoplastic elastomers derived from plant oil and their "click-coupling" via TAD chemistry. *Green Chem.* **2015**, *17*, 3806–3818.
(77) Martello, M. T.; Hillmyer, M. A. Polylactide–Poly(6-methyl-ε-caprolactone)–Polylactide Thermoplastic Elastomers. *Macromolecules* **2011**, *44*, 8537–8545.

(78) Martello, M. T.; Schneiderman, D. K.; Hillmyer, M. A. Synthesis and Melt Processing of Sustainable Poly(epsilon-decalactone)-block-Poly(lactide) Multiblock Thermoplastic Elastomers. *ACS Sustainable Chem. Eng.* **2014**, *2*, 2519–2526.
(79) Yu, Z.; Zhang, Q.; Li, L.; Chen, Q.; Niu, X.; Liu, J.; Pei, Q. Highly flexible silver nanowire electrodes for shape-memory polymer light-emitting diodes. *Adv. Mater.* **2011**, *23*, 664–668.
(80) Deng, J. E.; Zhang, Y.; Zhao, Y.; Chen, P. N.; Cheng, X. L.; Peng, H. S. A Shape-Memory Supercapacitor Fiber. *Angew. Chem. Int. Ed.* **2015**, *54*, 15419–15423.
(81) Hu, J. L.; Meng, H. P.; Li, G. Q.; Ibekwe, S. I. A review of stimuli-responsive polymers for smart textile applications. *Smart Mater. Struct.* **2012**, *21*, 1–23.
(82) Sisson, A. L.; Ekinci, D.; Lendlein, A. The contemporary role of epsilon-caprolactone chemistry to create advanced polymer architectures. *Polymer* **2013**, *54*, 4333-4350.
(83) Zhou, J. W.; Schmidt, A. M.; Ritter, H. Bicomponent Transparent Polyester Networks with Shape Memory Effect. *Macromolecules* **2010**, *43*, 939-942.
(84) Garle, A.; Kong, S.; Ojha, U.; Budhlall, B. M. Thermoresponsive Semicrystalline Poly(epsilon-caprolactone) Networks: Exploiting Cross-linking with Cinnamoyl Moieties to Design Polymers with Tunable Shape Memory. *ACS Appl. Mater. Interfaces* **2012**, *4*, 645-657.
(85) Lowe, J. R.; Tolman, W. B.; Hillmyer, M. A. Oxidized Dihydrocarvone as a Renewable Multifunctional Monomer for the Synthesis of Shape Memory Polyesters. *Biomacromolecules* **2009**, *10*, 2003-2008.
(86) Nagata, M.; Sato, Y. Synthesis and properties of photocurable biodegradable multiblock copolymers based on poly(epsilon-caprolactone) and poly(L-lactide) segments. *J. Polym. Sci., Part A: Polym. Chem.* **2005**, *43*, 2426-2439.
(87) Kutikov, A. B.; Reyer, K. A.; Song, J. Shape Memory Performance of Thermoplastic Amphiphilic Triblock Copolymer poly(D,L-lactic acid-co-ethylene glycol-co-D,L-lactic acid) (PELA)/Hydroxyapatite Composites. *Macromol. Chem. Phys.* **2014**, *215*, 2482-2490.
(88) Fan, X. S.; Tan, B. H.; Li, Z. B.; Loh, X. J. Control of PLA Stereoisomers-Based Polyurethane Elastomers as Highly Efficient Shape Memory Materials. *ACS Sustainable Chem. Eng.* **2017**, *5*, 1217-1227.
(89) Guo, B. C.; Chen, Y. W.; Lei, Y. D.; Zhang, L. Q.; Zhou, W. Y.; Rabie, A. B. M.; Zhao, J. Q. Biobased Poly(propylene sebacate) as Shape Memory Polymer with Tunable Switching Temperature for Potential Biomedical Applications. *Biomacromolecules* **2011**, *12*, 1312-1321.
(90) Migneco, F.; Huang, Y. C.; Birla, R. K.; Hollister, S. J. Poly(glycerol-dodecanoate), a biodegradable polyester for medical devices and tissue engineering scaffolds. *Biomaterials* **2009**, *30*, 6479-6484.
(91) Shearouse, W. C.; Lillie, L. M.; Reineke, T. M.; Tolman, W. B. Sustainable Polyesters Derived from Glucose and Castor Oil: Building Block Structure Impacts Properties. *ACS Macro Lett.* **2015**, *4*, 284-288.
(92) Guo, W. S.; Kang, H. L.; Chen, Y. W.; Guo, B. C.; Zhang, L. Q. Stronger and Faster Degradable Biobased Poly(propylene sebacate) as Shape Memory Polymer by Incorporating Boehmite Nanoplatelets. *ACS Appl. Mater. Interfaces* **2012**, *4*, 4006-4014.
(93) Hu, J. L.; Zhu, Y.; Huang, H. H.; Lu, J. Recent advances in shape-memory polymers: Structure, mechanism, functionality, modeling and applications. *Prog. Polym. Sci.* **2012**, *37*, 1720–1763.
(94) Gautrot, J. E.; Zhu, X. X. Shape Memory Polymers Based on Naturally-Occurring Bile Acids. *Macromolecules* **2009**, *42*, 7324-7331.

(95) Zotzmann, J.; Behl, M.; Feng, Y.; Lendlein, A. Copolymer Networks Based on Poly(ω-pentadecalactone) and Poly(ϵ-caprolactone)Segments as a Versatile Triple-Shape Polymer System. *Adv. Funct. Mater.* **2010**, *20*, 3583–3594.
(96) Katzenberg, F.; Heuwers, B.; Tiller, J. C. Superheated Rubber for Cold Storage. *Adv. Mater.* **2011**, *23*, 1909–1911.
(97) Guo, M.; Pitet, L. M.; Wyss, H. M.; Vos, M.; Dankers, P. Y. W.; Meijer, E. W. Tough Stimuli-Responsive Supramolecular Hydrogels with Hydrogen-Bonding Network Junctions. *J. Am. Chem. Soc.* **2014**, *136*, 6969–6977.
(98) Lewis, C. L.; Meng, Y.; Anthamatten, M. Well-Defined Shape-Memory Networks with High Elastic Energy Capacity. *Macromolecules* **2015**, *48*, 4918–4926.
(99) Wang, W.; Jin, Y.; Ping, P.; Chen, X. S.; Jing, X. B.; Su, Z. H. Structure Evolution in Segmented Poly(ester urethane) in Shape-Memory Process. *Macromolecules* **2010**, *43*, 2942-2947.
(100) Mohr, R.; Kratz, K.; Weigel, T.; Lucka-Gabor, M.; Moneke, M.; Lendlein, A. Initiation of shape-memory effect by inductive heating of magnetic nanoparticles in thermoplastic polymers. *Proc. Natl. Acad. Sci. U. S. A.* **2006**, *103*, 3540–3545.
(101) Xie, T. Recent advances in polymer shape memory. *Polymer* **2011**, *52*, 4985–5000.
(102) Neffe, A. T.; Hanh, B. D.; Steuer, S.; Lendlein, A. Polymer Networks Combining Controlled Drug Release, Biodegradation, and Shape Memory Capability. *Adv. Mater.* **2009**, *21*, 3394–3398.
(103) Li, Y.; Pruitt, C.; Rios, O.; Wei, L.; Rock, M.; Keum, J. K.; McDonald, A. G.; Kessler, M. R. Controlled Shape Memory Behavior of a Smectic Main-Chain Liquid Crystalline Elastomer. *Macromolecules* **2015**, *48*, 2864–2874.
(104) Zhou, J.; Turner, S. A.; Brosnan, S. M.; Li, Q.; Carrillo, J.-M. Y.; Nykypanchuk, D.; Gang, O.; Ashby, V. S.; Dobrynin, A. V.; Sheiko, S. S. Shapeshifting: Reversible Shape Memory in Semicrystalline Elastomers. *Macromolecules* **2014**, *47*, 1768–1776.